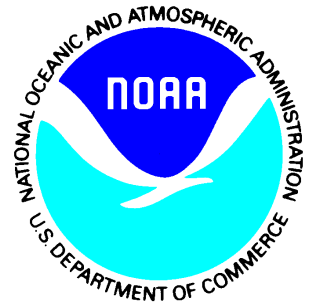

Satellite Products and Services Review Board

Algorithm Theoretical Basis Document

Enterprise Binary Snow Map Product



Version 1.0

June 2020

TITLE: ALGORITHM THEORETICAL BASIS DOCUMENT: ENTERPRISE BINARY SNOW
COVER PRODUCT

AUTHOR:

Peter Romanov (NOAA-CREST, City University of New York)

TABLE OF CONTENTS

	<u>Page</u>
LIST OF TABLES AND FIGURES	6
1. INTRODUCTION.....	7
1.1. Product Overview.....	7
1.1.1. Product Description	7
1.1.2. Product Requirements.....	8
1.2. Satellite Instrument Description.....	8
2. ALGORITHM DESCRIPTION	10
2.1. Processing Outline.....	10
2.2. Algorithm Input	10
2.3. Theoretical Description	13
2.3.1. Physical Description	13
2.3.2. Mathematical Description	21
2.4. Algorithm Output	22
2.5. Performance Estimates.....	242
2.5.1. Test Data Description.....	22
2.5.2. Sensor Effects	22
2.5.3. Retrieval Errors.....	23
2.6. Practical Considerations	297
2.6.1. Numerical Computation Considerations.....	297
2.6.2. Programming and Procedural Considerations	297
2.6.3. Quality Assessment and Diagnostics	297
2.6.4. Exception Handling.....	297
2.7. Validation.....	297
3. ASSUMPTIONS AND LIMITATIONS.....	318
3.1. Performance Assumptions	28
3.2. Potential Improvements	318
4. REFERENCES.....	329

LIST OF TABLES AND FIGURES

	<u>Page</u>
Table 1-1– Enterprise Binary Snow Cover product requirements	8
Table 2-1– Primary sensor input to Binary Snow Cover algorithm	11
Table 2-2– Derived products used by the Enterprise Binary Snow Cover algorithm	11
Table 2-3– Input static datasets used by the Binary Snow Cover algorithm.....	12
Figure 2-1– Snow frequency of occurrence (left) and snow cover probability (right) for week 5 of the year derived from NOAA weekly snow cover charts for 1972-1998.	13
Figure 2-2– ISCCP mean land surface (skin) temperature for the month of July	13
Figure 2-3– Spectral reflectance of natural surfaces and clouds.....	14
Figure 2-4– Spectral reflectance of snow covered forest, mountains and grassy plains	17
Figure 2-5– Snow surface temperature threshold	18
Figure 2-6– Global daily snow cover map derived with VIIRS on April 10, 2014 (left) and January 6, 2015 (right)	23
Table 2-4 Binary and Fractional Snow Map output parameters.....	21
Table 2-5 Snow Map Quality Information.....	21
Figure 2-7– VIIRS binary snow cover map with NOAA IMS data overlaid. April 14, 2014.	264
Table 2-6– Statistics of comparison of VIIRS and IMS snow maps.....	264
Figure 2-7– VIIRS binary snow cover map with NOAA IMS data overlaid. April 14, 2014.	275
Table 2-7– Statistics of comparison of VIIRS snow retrievals with station data in January 2015	286

1. INTRODUCTION

Snow and ice cover are among the key Earth's surface characteristics influencing radiation budget, energy exchange between the land surface or ocean and the atmosphere, and water balance. Information on the spatial extent and distribution of snow and ice cover presents an important input to numerical weather prediction (NWP), hydrological and climate models. Satellites present one of important sources of information on snow. High spatial resolution, wide area coverage and short revisit time allow for efficient, spatially detailed monitoring of both seasonal and perennial snow cover over the globe.

A large number of existing and future satellite sensors onboard operational polar orbiting and geostationary weather satellites provide daily observations of the Earth's surface in the visible, near-infrared, shortwave infrared, middle infrared and in the far infrared spectral bands. Observations with this set of spectral bands is sufficient for establishing an automated algorithm for snow cover identification and hence for providing routine mapping and monitoring of the global snow cover. Global daily observations are available at high, up to 375m spatial resolution from polar orbiting satellites and at up to 1 km resolution from geostationary satellites. This allows for detailed characterization of the snow cover distribution on the ground surface with remote sensing data.

This document presents the description of the Enterprise Binary Snow Cover product and of the corresponding Enterprise Binary Snow retrieval algorithm. This is a universal algorithm that is supposed to be used with observations from all operational polar orbiting and geostationary satellites at NESDIS. At this time the algorithm is applied to observations from the Visible Infrared Imaging Radiometer Suite (VIIRS) onboard SNPP and JPSS satellites. In the future it will be also used with the data from MetImage instrument onboard METOP Second Generation (SG) satellites. The Enterprise Binary Snow Cover algorithm is also planned for implementation with the Advanced Baseline Imager (ABI) of GOES-R series geostationary satellites, however in the latter case a number of modifications will be needed accounting for a completely different observation geometry.

1.1. Product Overview

1.1.1. Product Description

The Enterprise Binary Snow Cover Map Product provides binary (snow or no-snow) characterization of the land surface within the instrument field of view. The spatial resolution of the product matches the spatial resolution of the sensor data. It equals to 375m for VIIRS, 500m for MetImage and 1-2 km for ABI. Snow is identified only in the

satellite image pixels over the land surface. Given that most clouds are opaque in the visible and infrared spectral range, snow retrievals are performed only in clear sky conditions (no clouds within the instrument field of view). Since the algorithm relies on observations in the reflective bands, daytime conditions are required for snow retrievals. Besides the binary snow cover map, the product includes a quality flags file which provides support information on the quality of snow retrievals. The Enterprise Binary Snow Map product is delivered in NetCDF format.

1.1.2. Product Requirements

The requirements specified for the Enterprise Binary Snow Cover product are summarized in Table 1.1. For VIIRS the requirements are provided in GSegDPS (2019). The snow cover is identified in clear sky conditions during daytime (at less than 85 degree solar zenith angle). Retrievals are performed at 375m spatial resolution with VIIRS data and at 500m with MetImage. Snow retrievals should provide at least 90% or correct scene typing.

Table 1-1– Enterprise Binary Snow Cover product requirements

Name	Geographic Coverage	Horizontal Res.	Mapping Accuracy	Measurement Range	Measurement Accuracy (probability of correct typing)	Temporal Coverage Qualifier	Other Conditions Qualifier
Snow Cover	Global	VIIRS: 375m MetImage:500m	1 km	Binary yes/no detection	> 90%	Sun at 85 degree solar zenith angle	Clear sky conditions, over climatologically snow-covered regions

1.2. Satellite Instrument Description

VIIRS

The Visible Infrared Imaging Radiometer Suite (VIIRS) onboard SNPP and JPSS satellites is a multiband imaging instrument designed to support the acquisition of high-resolution atmospheric imagery and generation of a variety of applied environmental products characterizing the Earth's, atmosphere, oceans, land surface and cryosphere. VIIRS provides spectral observations within 412 nm to 12 μm in 16 bands at moderate spatial resolution of (~750 m at nadir), in a broadband optical moderate resolution day and night band (DNB) and high spatial resolution imagery at ~375 m in nadir in 5 spectral bands centered in the visible, near infrared, shortwave infrared, middle infrared and far infrared spectral range (VIIRS, 2013). As the satellite orbits the Earth, VIIRS scans a swath with the width of about 3040 km. This allows for a complete coverage of the Earth's surface at least

two times a day, on ascending and descending node. Observations data are delivered in granules of ~85 seconds long which cover the area of ~3040 by ~570 km in size. The SNPP and JPSS equator crossing time is about 1:30 local time.

MetImage

MetImage is a multispectral (visible and infrared) imaging passive radiometer for METOP SG satellite series. The instrument has 20 spectral bands covering the spectral range from 0.443 to 13.345 μm . It provides across-track scanning of the swath ~2670 km wide with a constant spatial sampling angle across the scan and a spatial resolution of 500m at nadir. Observations from MetImage will be delivered in the form of granules with the size of granules TBD. The planned launch date for METOP SG A and B satellites is 2023 and 2024 respectively. The equator crossing time for METOP satellites is about 9:30 local time.

2. ALGORITHM DESCRIPTION

This section presents the detailed description of the algorithm to generate the Enterprise Binary Snow Cover product.

2.1. Processing Outline

The Enterprise Binary Snow Cover algorithm provides discrimination between snow-covered and snow-free land scenes. Snow cover in the sensor field of view is identified using a two-step algorithm. First, a preliminary snow identification is performed through a pixel-by-pixel spectral-based classification of the satellite image. Second, pixels identified as “snow covered” in the preliminary classification are subjected to a series of consistency tests to identify and properly label potential spurious snow.

The Enterprise Binary Snow Cover algorithm is based on earlier snow detection and mapping algorithms developed for EOS MODIS by NASA (Hall et al, 2003) , GOES Imager (Romanov et al., 1999, 2003), and NOAA AVHRR (Romanov, 2014). GOES Imager and NOAA AVHRR algorithms are currently implemented operationally at NESDIS OSDPD as part of the Global Multisensor Snow and Ice Mapping System (GMAI-Autosnow).

At this time cloud masking is not performed by the Enterprise Binary Snow Cover algorithm: Information on the cloud cover is obtained from the Cloud Mask product which presents an external input to the Binary Snow Cover algorithm and is assumed to be available at the time of snow retrieval. The algorithm also relies on the external land/water mask to identify land cover where snow identification is performed. Pixels identified as “water” in the land/water mask are not processed by the algorithm.

2.2. Algorithm Input

The Enterprise Binary Snow Cover algorithm input includes sensor and ancillary input data. The ancillary data include both satellite-derived data and static datasets.

Table 2-1 provides information on the primary sensor input to the algorithm. At this time as the input the algorithm uses observations in the visible, near infrared, shortwave infrared and far infrared spectral bands. In the future modifications of the algorithm possible application of the middle infrared spectral band data is assumed. Additional sensor input data include Latitude, Longitude of the pixel along with the observation geometry characterized by the Solar Zenith Angle, Satellite View Angle and Solar-Satellite Relative Azimuth. Observation geometry angles are specified for each satellite image pixel.

Table 2-1– Primary sensor input to Enterprise Binary Snow Cover algorithm

Spectral Band	VIIRS Band (resolution, m)	VIIRS Central Wavelength (μm)	MetImage Band (resolution, m)	MetImage Central Wavelength(μm)	Input Type
Visible	I1(375m)	0.640	VII-12 (500m)	0.668	Current
Near IR	I2(375m)	0.865	VII-17 (500m)	0.865	Current
Shortwave IR	I3(375m)	1.61	VI-24 (500m)	1.63	Current
Mid-IR	I4(375m)	3.740	VI-26 (500m)	3.74	Expected Added
Therma IR	I5(375m)	11.45	VI-37 (500m)	10.69	Current

Other derived satellite data used by the algorithm include the Cloud Mask (including cloud shadow flag) (see Table 2-2). Within the data processing chain, the Cloud Mask is supposed to be derived prior to the Binary Snow Cover product.

Table 2-2– Derived satellite products used by the Enterprise Binary Snow Cover algorithm

Name	Description	Dimension
Cloud Mask	4-category cloud mask	Granule

There are several environmental static datasets that are also utilized in the Binary Snow Cover product. These datasets are listed in Table 2-3 and include the land-water mask, surface elevation, snow cover climatology, land surface temperature climatology and the algorithm control parameters data file.

Land-water mask and surface elevation are specified at the granule level and are defined for every satellite image grid cell, whereas the snow cover climatology and the land surface temperature are defined at a coarser spatial resolution.

Table 2-3– Input static datasets used by the Binary Snow Cover algorithm

Name	Description	Dimension
Land/Water Mask	Binary file discriminating land and water-covered pixels	Granule
Surface elevation	Binary file specifying surface elevation for every pixel of the granule	Granule
Snow Cover Climatology	Weekly maps of snow cover frequency of occurrence on 1/3 degree global lat/lon grid.	1080x540 (0.33° x 0.33°)
Land Surface Temperature Climatology	Monthly mean land surface temperature	144x72 (2.5° x 2.5°)
Algorithm Control Parameters	Threshold values and other parameters controlling the VIIRS image classification (snow detection) algorithm.	

The snow cover climatology is presented as the weekly snow cover occurrence probability. Climatic information on the snow cover occurrence has been derived from NOAA weekly interactive snow and ice charts produced during the time period from 1972 to 1998. This is so far the longest time period when the spatial resolution of the maps remained unchanged. The spatial resolution of NOAA weekly snow charts generated during that time was about 180 km. From 1998 to 2004 the IMS snow charts were produced daily at about 24 km resolution, whereas in 2004 the spatial resolution was increased to 4 km (Helfrich, 2007). Therefore, the whole 40+ year long time series of NOAA Interactive snow product cannot be considered homogeneous.

To estimate the probability of snow occurrence weekly NOAA snow charts over the 26-years long time period (1972-1998) were regridded to 30 km latitude-longitude grids and the frequency of occurrence of snow cover for each week was calculated. Every grid cell of each weekly map was then assigned one of three categories named “snow unlikely”, “snow possible” (or “intermittent snow”) and “persistent snow” depending on the frequency of occurrence of the snow cover in that particular grid cell and in its close proximity. The grid cell was labeled as “snow possible” if on the current, preceding or subsequent week the estimated snow cover frequency of occurrence in any of the grid cells within the 200 km radius from the current grid cell ranged from 1% to 99%. All remaining grid cells with the frequency of occurrence of 0% or 100% were labeled correspondingly as “snow unlikely” and “persistent snow”. Figure 2-1 presents an example of a weekly map of snow cover

frequency of occurrence and a corresponding map of snow cover probability classes (“persistent snow”, “snow possible” and “snow unlikely”). Since NOAA snow and ice charts are produced only over the Northern Hemisphere, the derived snow cover occurrence statistics is available only south of the equator.

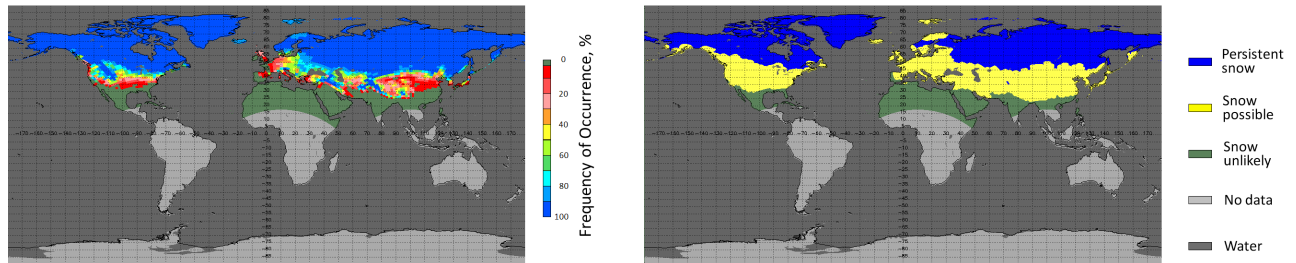


Figure 2-1– Snow frequency of occurrence (left) and snow cover probability (right) for week 5 of the year derived from NOAA weekly snow cover charts for 1972-1998.

The land surface temperature climatology is based on the data of the International Satellite Cloud Climatology Project (ISCCP). Monthly mean surface temperature is specified within 2.5x2.5 degree grid cells. Data are available from ISCCP anonymous ftp site at <ftp://isccp.giss.nasa.gov/pub/data/surface/>. As an example, Figure 2-2 presents the global mean temperature for the month of July.

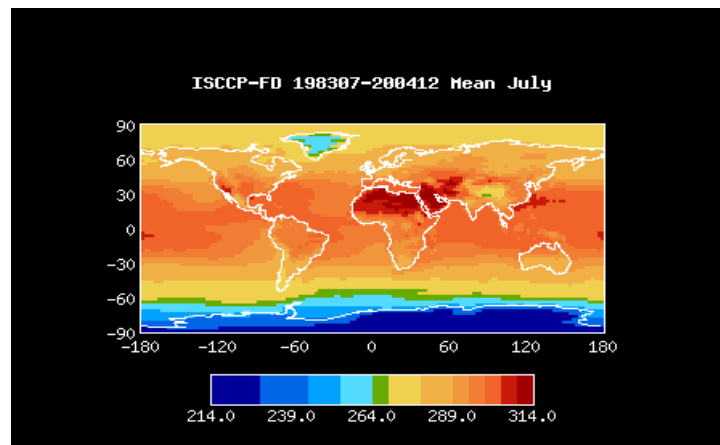


Figure 2-2– ISCCP mean land surface (skin) temperature for the month of July

2.3. Theoretical Description

2.3.1. Physical Description

Physical Basis

Automated identification of snow-covered land surface from space is based on a specific spectral reflectance signature of snow. The reflectance of snow drops from high values, up to 90-95%, in the visible spectral band to low values below 20% in the shortwave and in the middle infrared spectral band (see Figure 2-3). This spectral pattern of snow cover reflectance is different from spectral reflectance of most natural land surface cover types (e.g., soil, water, vegetation) which typically appear much “darker” in the visible band. In the far infrared spectral band, snow emits thermal radiation close to that of a blackbody and thus its brightness temperature as observed by the satellite sensor depends mainly on the physical temperature of the top thin layer of the snow pack. At these wavelengths, the snow brightness temperature is relatively low, which is also a useful feature for the remote snow identification.

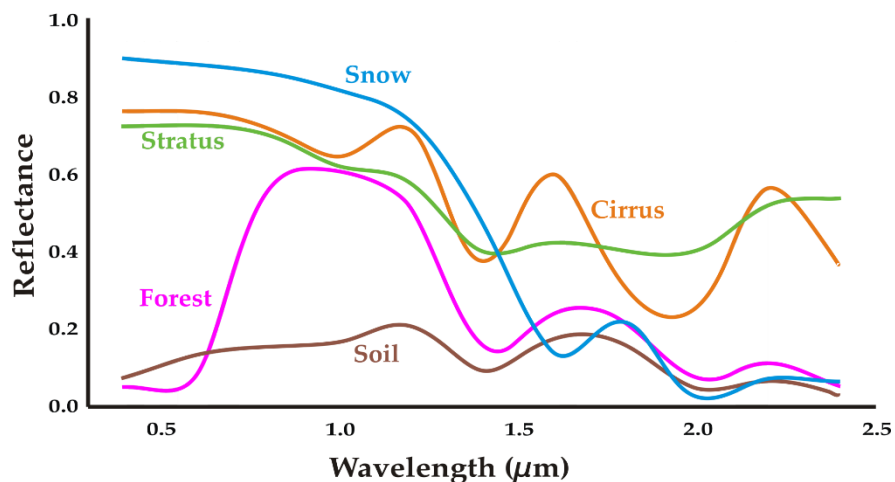


Figure 2-3– Spectral reflectance of natural surfaces and clouds

Most clouds are opaque in the visible and infrared spectral bands. Liquid-phase clouds typically exhibit high reflectance both the visible and in the shortwave infrared bands. High reflectance in the visible band along with colder infrared brightness temperature discriminates clouds from snow-free land surface, whereas their high reflectance in the shortwave infrared differentiates clouds from the snow-covered land surface.

Both VIIRS and Metlge, as well as most current instruments onboard meteorological polar orbiting and geostationary satellites, have spectral channels centered in the visible at around 0.6 μm, near-infrared at 0.9 μm, shortwave-infrared at 1.6 μm, middle infrared at 3.7 μm - 3.9 μm, and in the thermal infrared at 10 μm -12 μm and thus provide observations

in these bands. These spectral bands are generally sufficient to distinguish snow from most clouds and from the snow-free land surface in the satellite imagery and therefore could be used for mapping snow cover with an automated algorithm. Practical solutions to discriminate between snow, snow-free land and clouds in satellite imagery with an automated technique could be different.

Heritage algorithms

Most automated (or unsupervised) algorithms to identify snow usually incorporate a set of threshold tests or criteria that utilize satellite-observed reflectance and brightness temperature values in the spectral bands mentioned above as well as various spectral indices. Spectral indices are utilized to characterize the spectral gradient of the scene reflectance or brightness temperature and can be defined as ratios, differences or normalized differences of the observed reflectance or brightness temperatures at two, or, sometimes, three, wavelengths. In particular, in the snow identification algorithm developed for the Imager instrument onboard GOES satellites (Romanov et al., 2000) snow is primarily identified using a snow index (SI), defined as a simple ratio of the TOA reflectance in the visible (R_{vis}) and in the middle infrared (R_{mir}). A similar index where R_{mir} is replaced by the observed reflectance in the shortwave infrared (R_{swir}) can also be used in snow detection schemes (e.g., Romanov et al, 2006).

The algorithm of Hall et al. (2002) to distinguish between snow-free and snow-covered pixels in the imagery of the Moderate Resolution Imaging Spectroradiometer (MODIS) onboard NASA Terra and Aqua uses the normalized difference between TOA reflectance observed satellites in the visible spectral band at $0.6 \mu\text{m}$ (R_{vis}) and in the shortwave infrared spectral band at $1.6 \mu\text{m}$ (R_{swir}). The index is referred to as the Normalized Difference Snow Index (NDSI) and is expressed as

$$NDSI = (R_{vis} - R_{swir}) / (R_{vis} + R_{swir})$$

Snow-free land surfaces typically exhibit lower values of SI and $NDSI$ than snow covered land. In the snow mapping algorithm of Hall et al. (2002), cloud-free pixels having $NDSI > 0.4$, a visible reflectance of over 11%, and infrared brightness temperature below 283K are classified as snow-covered.

There is a number of factors complicating snow identification in satellite imagery and hampering generation of accurate maps of the snow cover distribution. One of these factors is vegetation which masks snow on the ground surface and thus reduces the visible reflectance of the scene. This effect is the strongest in densely forested areas which are associated with most misses of snow cover in satellite snow products. To account for the vegetation cover effects on the snow reflectance and to improve snow identification in

forests, snow identification algorithms of Hall et al (2002) incorporates the Normalized Difference Vegetation Index (NDVI)

$$NDVI = (R_{nir} - R_{vis}) / (R_{nir} + R_{vis}),$$

where R_{nir} is the scene reflectance in the spectral band centered in the near infrared part of spectrum at around 0.9 μm . At $NDVI$ values of over 0.2 indicating the presence of at least some green vegetation within the instrument field of view a lower NDSI threshold value down to 0.1 is used allowing more pixels to be classified as “snow covered”. $NDVI$, $NDSI$ and SI indices are incorporated in the snow mapping algorithm for METOP AVHRR within NESDIS Global Multisensor Automated Snow and Ice Mapping System, GMASI (Romanov, 2014). The current algorithm to identify snow in the VIIRS imagery is almost identical to the MODIS snow map algorithm (Key et al., 2013). It uses a combination of $NDSI$ and $NDVI$ indices for a preliminary identification of the snow cover and a visible reflectance and thermal tests to eliminate snow-free scenes that look spectrally similar to snow from being classified as “snow cover”

Post-launch modifications for the VIIRS snow detection spectral algorithm

The analysis of performance of the MODIS snow mapping algorithm as applied to the VIIRS data has shown that it tends to miss some partially snow-covered pixels and label them as “snow free”. Part of these misses occurs due to an excessively conservative $NDSI/NDVI$ test and part is due to a too low snow temperature threshold value. The conservative nature of the MODIS $NDVI-NDSI$ threshold tests is illustrated in Figure 2-4 showing the VIIRS-observed $NDVI$ and $NDSI$ values over snow-covered land surface for three land cover types, forest, mountains and grassy plains. As it follows from the example in Figure 2-4, the spectral response of a large portion of snow covered forest pixels and of some pixels in the snow-covered grassy plains does not fit into the threshold criteria set by the MODIS snow mapping algorithm (shown with the blue line in Figure 2-4) thus causing snow misses. For the JPSS VIIRS snow mapping algorithm we proposed a more liberal $NDVI-NDSI$ criteria (shown with a black line in Figure 2-4), which better characterizes the range of spectral response from snow-covered scenes and therefore should provide more accurate identification of snow-covered pixels.

The analysis of the snow cover mapping results in the mountains has revealed frequent misses of snow at the boundary of the snow-covered area due to a low temperature threshold value of 283K. Pixels with larger infrared brightness temperature were automatically classified as snow-free. A larger threshold value was found to provide more adequate mapping of the snow cover. An example in Figure 2-5 demonstrates the effect of changing the temperature threshold value from 283K to 290K on the mapped snow cover. The value of 290K is incorporated in the AVHRR-based snow detection algorithm within the GMASI system (Romanov, 2014). For the MODIS Collection 6 snow products, the

temperature screen is not applied at all. However we have found that elimination of this test completely may cause false snow identifications due to misinterpretation of dry sandy areas as snow covered. For the VIIRS snow mapping algorithm we have set the temperature threshold value to 285K. It was found that further increasing the threshold value causes propagation of a considerable number of snow false detections into the product.

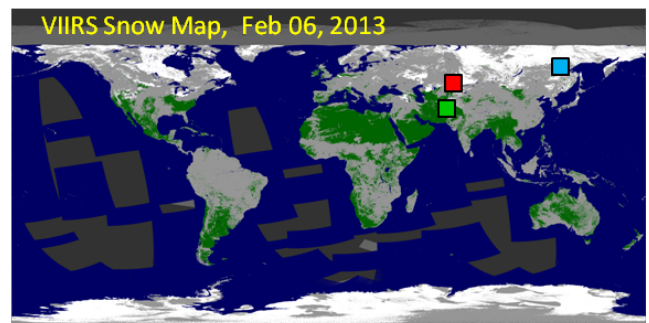
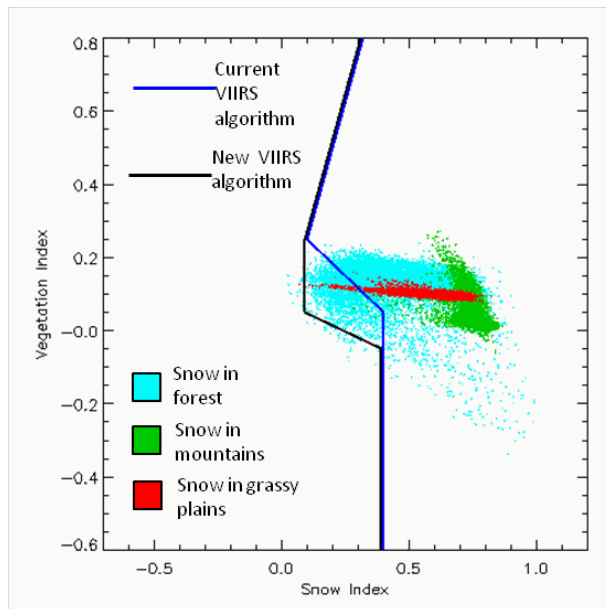


Figure 2-4– Spectral reflectance of snow covered forest, mountains and grassy plains

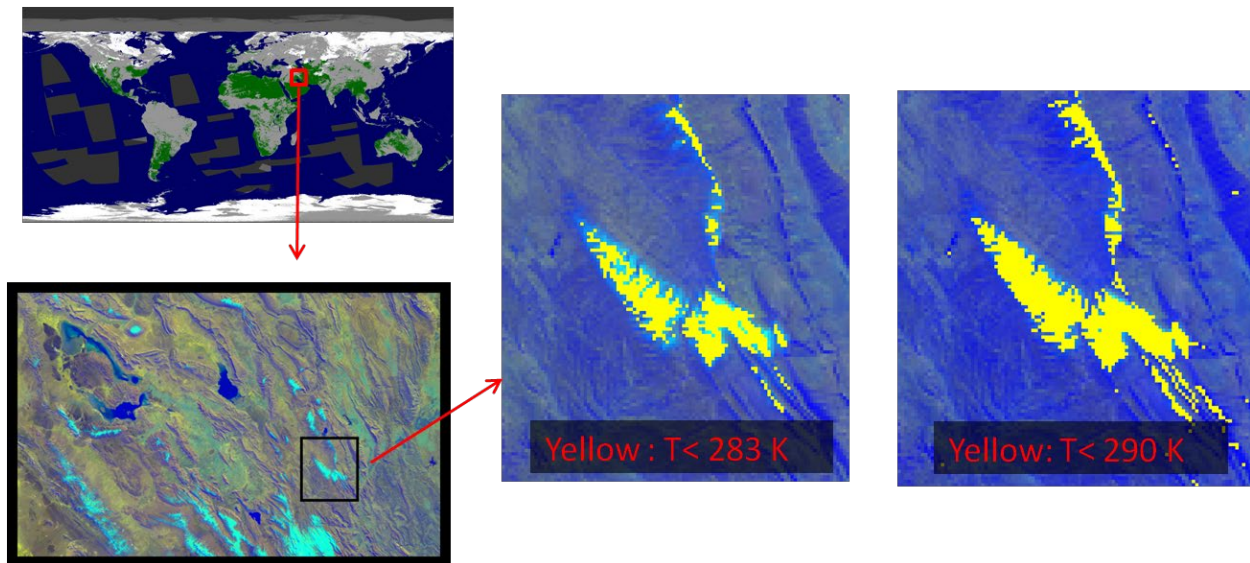


Figure 2-5– VIIRS snow temperature threshold

To further improve snow identification we introduced two additional threshold tests involving the observed reflectance in the shortwave infrared band 13 (R_3) and calculated reflectance in the middle infrared band 4 (R_4). To be classified as “snow” the pixel reflectance in these bands is required to be less than the threshold values. At this time the threshold values for R_3 and R_4 are set correspondingly to 0.25 and 0.05.

The analysis of the VIIRS imagery have shown that the visible reflectance threshold of 0.11 adopted in the MODIS algorithm may be too high for VIIRS. Large snow covered areas, particularly forested areas, in the VIIRS imagery exhibit the visible reflectance below 0.11. Moreover, the reflectance of the snow covered forest has been found to vary with the observation geometry and solar illumination angle. Therefore, in the VIIRS algorithm some modifications were introduced to the visible threshold value. The basic threshold value was set to 0.05, however it may increase with increasing solar and satellite zenith angle, increasing NDVI and for high values of surface temperature. In particular the NDVI additive corrective factor to R_1 was set to increase linearly from 0 to 0.02 for NDVI increasing from 0 to 0.5. The temperature corrective factor increases linearly from 0 to 0.05 for IR surface temperature increasing from 270 to 280K, while the geometry-related corrective factor is expressed as

$$dR_{1g} = a_1 (1-\cos(\Theta_{sat}))^2 + a_2 (1-\cos(\Theta_{sol}))^2 + a_3 (1-\cos(\Theta_{sat}))(1-\cos(\Theta_{sol}))^2 ,$$

where Θ_{sat} and Θ_{sol} are satellite and solar zenith angle respectively. The maximum cumulative additive correction to the threshold value of the R_1 can theoretically reach 0.1, but in practice typically range within 0.01-0.05.

In the developed algorithm the threshold values and parameters controlling the corrective factors are flexible and may be changed in the future to provide more accurate snow mapping.

Planned modifications for the METOP SG MetImage snow detection spectral algorithm

The Enterprise Binary Snow identification algorithm will be applied to METOP SG Met Image data. However given that the current algorithm has been developed for VIIRS and that spectral bands of METImage are somewhat different from corresponding bands of VIIRS (see Table 2-1) we expect that some modification to the original algorithm may be needed. These modifications will concern the particular threshold values controlling the performance of threshold-based snow identification tests. Updates to the threshold values incorporated in the Binary Snow algorithm for MetImage will be introduced once the simulated MetImage data will be available. Further updates should be assumed once operational data from METOP SG MetImage become available. Prelaunch MetImage algorithm testing and evaluation will be performed with original threshold values determined for SNPP and JPSS VIIRS.

Planned modifications for GOES-R ABI Binary Snow detection algorithm

The spectral threshold-based snow detection algorithm developed and implemented for VIIRS may generally be applied to observations from ABI observations from GOES-R series satellites. However, besides somewhat different spectral bands of ABI, the viewing-illumination geometry of observations from geostationary satellites is different from the observation geometry inherent to sensors onboard polar-orbiting satellites. Whereas observations from polar orbiting satellites with the equator crossing time close to local noon are mostly characterized by cross-principal plane observations geometry, observations from geostationary satellites over snow-covered land both in the Northern and in the Southern Hemisphere are performed predominantly in the backscatter geometry.

Furthermore, the satellite view angle of geostationary satellite observations varies within the whole, 0 to 90 deg range. Observations in the backscatter taken at high view and illumination zenith angles may be strongly affected by specular reflectance from clouds and mountain ice caps. In the visible band and to a lesser extent in longer wavelength bands, the reflectance observed from geostationary satellites have a large contribution of diffuse radiation due to scattering in the atmosphere. Therefore, adjusting the Enterprise Binary Snow algorithm for ABI will require both modification of algorithm spectral threshold values

and setting additional retrieval exclusion conditions to avoid using the algorithm with observations that are hard to properly interpret.

Additional consistency tests

The primary source for snow false identifications are clouds missed by the cloud masking algorithm. Spectral features of many types of clouds resemble the ones of snow, thus it is very likely that missed clouds are interpreted as snow by the snow identification algorithm and hence contribute to the snow commission error. Our analysis of satellite imagery has shown that some other surface types can also exhibit the spectral response similar to snow. The latter includes in particular wet salars and snow-free forested scenes affected by smoke from fires. Since it is impossible to discriminate these scenes from the snow cover using spectral features other tests involving independent datasets and the analysis of the consistency of the spatial pattern of mapped clouds and snow should be applied.

We have developed a number of such tests with the intent to identify and eliminate potential false snow identifications. The developed tests include (1) Temperature climatology test, (2) Snow climatology test, (2) Isolated snow pixel test, (3) Temperature spatial homogeneity test, (4) Snow small cluster filter and (5) Cloud neighbor filter. All tests are applied only to pixels classified as “snow” by the spectral-based algorithm. Pixels that pass all these tests are flagged as “confirmed snow”. All “potential snow” pixels that fail at least one test are labeled as “unconfirmed snow”. Details of all filters are given below.

(1) Temperature Climatology Test

Within this test the pixel IR brightness temperature value observed in the thermal infrared band of the sensor (T_{IR}) is compared with the multiyear mean (climate) value of the land surface temperature (LST) for the pixel location for given time of the year. The climatic LST is corrected for the elevation of the pixel assuming a 7 degC/km vertical temperature gradient. If the observed T_{IR} is over 20K below the climatic LST, “snow” is rejected and the pixel is labeled as cloudy. The test uses monthly LST climatology developed as part of the ISCCP project. To estimate the climatic LST value for a given day a linear interpolation is performed between LST values for the two consecutive months. When performing interpolation monthly climatic LST values are assumed valid for the 15th day of the month.

(2) Isolated Snow Pixel Test

Misclassifications of clouds as snow most often appear as isolated “snow” pixels in the midst of clouds. To eliminate these misclassifications a 3x3 pixel sliding window is used to locate isolated “snow” pixels completely surrounded by cloudy pixels. If all eight pixels next to the “snow” pixel in the 3x3 box are cloudy, the “snow” pixel is rejected and is labeled as cloudy.

(3) Temperature Spatial Homogeneity Test

The idea of this test is to check whether there are any pixels in the neighborhood of the "snow" pixel that are much warmer than the "snow" pixel. Outside of mountainous areas and large water bodies the spatial gradient of the land surface temperature is limited. Therefore, a substantial number of much warmer pixels may indicate that identification of "snow" is erroneous. For this test a sliding window of ~100x100 km (51 x 51 grid cells) centered at the "snow" pixels is applied. Within this region we identify the pixels whose IR brightness temperature in the thermal IR sensor band the corresponding temperature of the "snow" pixel by more than 20K. The "snow" pixel is reassigned to the "cloud" category if the number of these much warmer pixels found within the sliding window area exceeds 10 (or more than 0.4%). The test is not applied in high altitude areas with elevation above 900 m. It also does not account for the temperature of pixels covered by water for more than 30% or located more than 300m below the central "snow" pixel.

(4) Snow small cluster filter

A sliding window of 10x10 pixels (grid cells) is used to identify isolated small clusters of "potential snow" pixels in the midst of clouds. There is high likelihood that in these pixels clouds were falsely classified as snow. If all pixels on the window perimeter are cloudy and the fraction of clear pixels is less than 15%, pixels previously identified as "snow" are reassigned a "cloudy" flag.

(5) Cloud neighbor filter

A 3x3 sliding window centered on a "snow" pixel is examined. If any other of the pixels within the box is cloudy, the "snow" pixel is labeled as "cloudy". The test is applied to all snow pixels with surface elevation below 500m. The surface elevation condition is added to retain capability to properly identify snow caps on mountains. As of June 2020 all consistency tests in the VIIRS operational snow mapping algorithm were turned on. We are also planning to use all developed consistency tests with MetImage data.

Settings incorporated in the software allow for turning on and off any or all of the tests. At the time of the algorithm testing and implementation all consistency tests were turned on.

2.3.2. Mathematical Description

The implemented algorithm follows the description provided in Section 2.3.1. Prior to the retrieval all input reflectances and brightness temperatures used by the algorithm are tested for validity. If any of the reflectance or brightness temperature values is invalid, the processing of the pixel data is terminated and the processing of the next pixel begins.

To ensure availability of adequate sunlight for the accurate image classification snow identifications are conducted only when the solar zenith angle does not exceed 85 degrees. Snow identification is attempted if pixel is classified as “confidently cloud clear” by the cloud mask and as “land” by the land/water mask.

Snow identification is performed in two steps, first spectral tests are applied and then consistency tests are activated. Spectral tests are applied on a pixel-by pixel basis where as consistency tests utilize a pixel-by pixel approach as well as the analysis of the image spatial patterns. Consistency tests are applied only to pixels which were classified as “snow covered” by the spectral algorithm. “Snow covered” pixels which are rejected by any of the consistency tests are labeled as “rejected snow” and a corresponding quality flag indicating which particular test was not passed is assigned.

2.4. Algorithm Output

SNPP and JPSS VIIRS Binary Snow product

The algorithm output for VIIRS includes the binary snow cover map, the quality flags associated with the map and metadata. The map and the quality flags present the arrays of the size corresponding to the size of the VIIRS granule. Metadata is a text file. The output is provided in NetCDF format. Figure 2-6 provides an example of daily global binary snow maps generated from all binary snow granules produced in the course of one day. Detailed description of the output is provided in Tables 2.4 and 2.5.

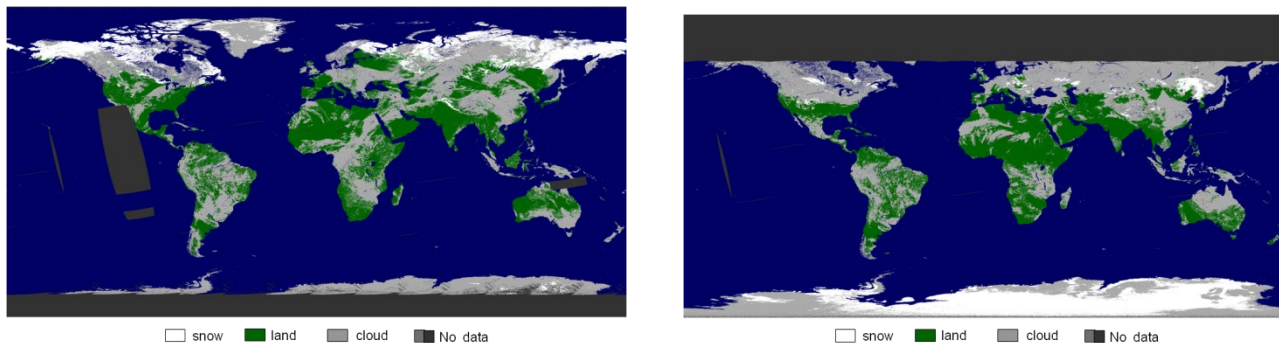


Figure 2-6– Global daily snow cover map derived with VIIRS on April 10, 2014 (left) and January 6, 2015 (right)

Table 2-4 Binary and Fractional Snow Map output parameters (1 byte)

Parameter	Description	Unit
Binary snow cover	Reports whether the pixel is snow-covered or snow-free Value 0 : Snow not identified 1: Snow identified 128: No retrieval	Unitless

Table 2-5 Snow Map Quality Information (1 byte)

Parameter	Description	Unit
Quality Flag	Provides product quality information Value 0 : Good retrieval 105: water 110: cloud 111: rejected snow due to inconsistency with snow climatology 112: rejected snow, inconsistent with surface temperature climatology 113: rejected snow, failed spatial consistency test 114: rejected snow, failed temperature uniformity test 121: night, insufficient solar illumination	Unitless

	122: undetermined 124: bad pixel SDR 125: fill value 128: No retrieval	
--	---	--

MetImage and ABI Binary Snow product

The format and the content of the Binary Snow cover product from MetImage and ABI will be defined once detailed requirements to the output product are formulated. Prior to that the output Binary Snow product from these two sensors will be the format and content identical to the one of VIIRS.

2.5. Performance Estimates

2.5.1. Test Data Description

Performance estimates of the algorithm for existing sensors (e.g., VIIRS) is performed with operationally acquired sensor data. These data allow for estimating the accuracy and performance of the algorithm over the whole globe and for different seasons. Performance of the snow algorithm with ABI data will also be assessed using operational observations. MetImage accuracy assessment will be conducted with simulated data first, and then, after the launch of METOP SG A, with real satellite observations.

2.5.2. Sensor Effects

Any sub-optimal performance of the satellite sensors may cause degradation of the quality of the binary snow cover retrievals. This concerns all sensors operating in the visible, near-infrared, shortwave infrared and thermal infrared bands which are directly used to identify snow in satellite imagery.

It is important that the Enterprise Binary Snow cover product relies on the cloud mask provided as input to the algorithm. Therefore, the excessive noise or inadequate calibration of sensors involved in the production of the cloud mask may adversely affect the accuracy of the Binary Snow Cover Map product.

Some geophysical phenomena causing a substantially reduced atmospheric transmittance in the visible, near infrared or shortwave infrared bands (e.g., smoke from fires or dust from volcanic eruptions) will also adversely affect snow retrievals. These phenomena can cause snow misses as well as false snow identifications depending on a particular scene, the fraction of snow on the ground and the observation geometry.

2.5.3. Retrieval Errors

Validation and accuracy assessment of the derived Enterprise Binary Snow cover maps is performed with two independent datasets: Interactive snow cover charts derived within the NOAA Interactive Multisensor Snow and Ice Mapping System (IMS) and in situ observations of the snow cover as reported by WMO and US Cooperative network stations. Both data sets are used qualitatively, by generating and examining overlays of the derived Binary Snow map with the independent snow products as well as through their quantitative comparison.

At this time the Enterprise Binary Snow algorithm is routinely used only with SNPP and JPSS-1 VIIRS observations. Therefore, a detailed analysis of snow retrieval errors is provided only for this sensor data. Performance and accuracy estimates of the Binary Snow product derived from MetImage and ABI will be added to the document later once the results of application are available.

The comparison of VIIRS Binary Snow retrievals with IMS has demonstrated their general consistency and good agreement. Figure 2.7 presents an overlay of the snow cover mapped by VIIRS and the snow map generated by IMS analysts. Except of small differences along the snow cover boundary and in the mountainous regions, the snow cover distribution mapped by VIIRS is qualitatively consistent with the IMS product.

The results of quantitative comparison of the two products are given in Table 2-6. To quantitatively compare the two products VIIRS data were gridded onto a simple latitude-longitude projection with 0.01 degree (or about 1 km) grid cell size. The comparison was performed over all Northern Hemisphere grid cells classified as "land" in both products. The overall agreement between daily products for the period covered by tests ranged generally from 96 to 99%. Most of the disagreement was due to snow omission errors in the VIIRS snow cover maps which accounted for 0.7 to 3.5% of all compared grid cells.

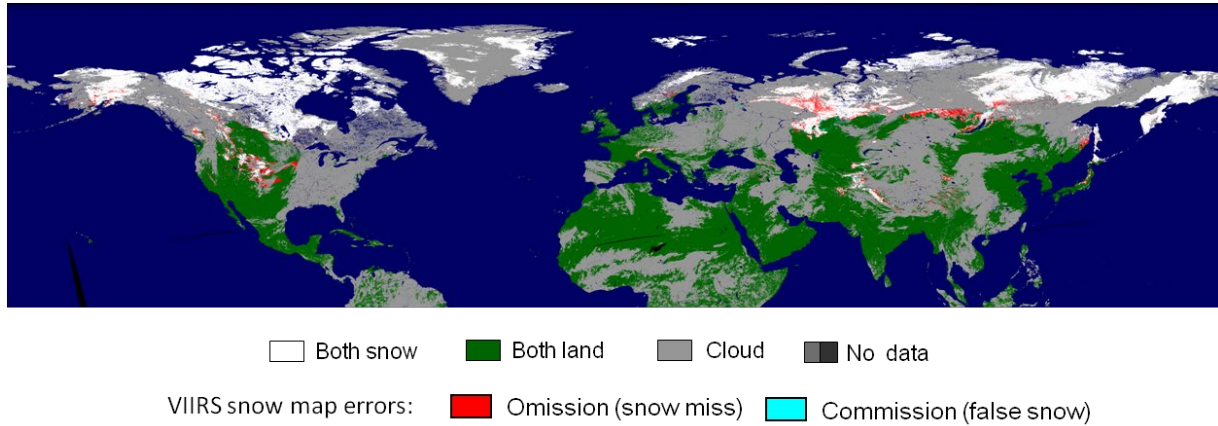


Figure 2-7– VIIRS binary snow cover map with NOAA IMS data overlaid. April 14, 2014.

Table 2-6– Statistics of comparison of VIIRS and IMS snow maps

Year	Day	Agree, %	Disagr, %	Snow Miss, %	False Snow, %	Cloudy, %
2014	100	96.8	3.2	2.7	0.5	51.9
2014	101	96.9	3.1	2.8	0.3	49.6
2014	102	97.4	2.6	2.2	0.4	49.7
2014	103	96.9	3.1	2.6	0.5	50.4
2014	104	97.1	2.9	2.5	0.3	47.5
2014	105	99.2	0.8	0.7	0.1	15.8
2014	191	97.8	2.2	0.9	1.3	60.4
2014	192	97.7	2.3	1	1.3	61.9
2014	193	97.9	2.1	1	1.1	64.1
2014	194	97.7	2.3	0.8	1.5	62.1
2014	195	97.8	2.2	0.8	1.5	61.4
2014	196	97.4	2.6	0.8	1.8	63.4
2014	283	97	3	1.9	1.1	51.8
2014	284	97.3	2.7	1.9	0.8	52.5
2014	285	97.1	2.9	2.2	0.7	51.5
2014	286	97.3	2.7	2	0.8	52.7
2014	287	97.9	2.1	1.7	0.4	50.2
2015	1	96.9	3.1	2.5	0.6	35.5
2015	2	96.5	3.5	2.9	0.6	32.9
2015	3	96.9	3.1	2.6	0.5	32.9
2015	4	97	3	2	1	32.2
2015	5	97.4	2.6	1.9	0.7	33.7
.....
2015	25	96.2	3.8	3.4	0.4	40.4
2015	26	96.1	3.9	3.5	0.4	40
2015	27	97.1	2.9	2.7	0.2	40.8
2015	28	97.3	2.7	2.2	0.5	40.4
2015	29	96.8	3.2	2.7	0.4	39.1
2015	30	97.1	2.9	2.5	0.3	40.6
2015	31	97.2	2.8	2.3	0.5	44.3

Comparison of VIIRS retrievals with in situ data was performed over Conterminous US (CONUS area). In this region besides snow observations at regular WMO stations, snow depth reports are also available from a large number of US Cooperative network stations. Figure 2-7 illustrates the spatial distribution and the density of the stations used in the VIIRS validation efforts. VIIRS snow maps with surface observations overlaid similar to the one presented in Figure 2-7 were routinely used to qualitatively examine the agreement between the two datasets.

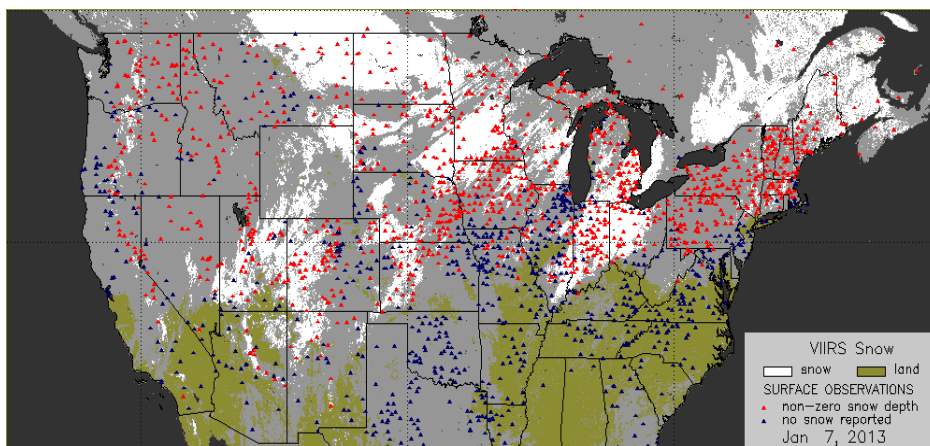


Figure 2-7– VIIRS binary snow cover map with NOAA IMS data overlaid. April 14, 2014.

The results of quantitative comparison of VIIRS snow maps with surface observations data in January 2015 are presented in Table 2-7. The agreement of VIIRS daily snow retrievals to the station data ranged within 88 to 97.4% with the mean value of 92.5%. In the comparison with station data the VIIRS commission and omission errors were more balanced with the mean frequency of occurrence of snow misses and false snow identifications of 3.2% and 4.3% correspondingly. It is important that part of the disagreement (up to about 1%) may be caused by errors in insitu snow depth reports which are not quality controlled.

The two experiments demonstrate that overall the accuracy of snow identification with the new VIIRS algorithm satisfies the requirements of 90% correct typing of the scene. More comprehensive estimates of the accuracy will be available once the algorithm is applied to the VIIRS data operationally and the daily binary snow cover maps are available routinely. Tuning the threshold values and improving the snow identification algorithm may bring some improvement to the snow mapping accuracy.

Table 2-7– Statistics of comparison of VIIRS snow retrievals with station data in January 2015

Year	Day	Match-ups	Agree %	Snow Miss, %	False Snow, %
2015	1	564	92.6	5.3	2.1
2015	2	460	90	6.7	3.3
2015	3	187	88.2	4.3	7.5
2015	4	335	92.8	4.8	2.4
2015	5	686	96.5	1	2.5
2015	6	567	94	1.9	4.1
2015	7	1051	91.8	4.9	3.3
2015	8	789	88.3	4.7	7
2015	9	920	93.7	2.6	3.7
2015	10	759	92.8	3.8	3.4
2015	11	221	93.7	4.1	2.3
2015	12	726	95.5	2.8	1.8
2015	13	1038	94.3	3.2	2.5
2015	14	609	90.8	3.6	5.6
2015	15	1280	92	3.8	4.1
2015	16	1047	91.7	3.4	4.9
2015	17	885	92.1	3.2	4.7
2015	18	850	90.1	3.6	6.2
2015	19	929	92.4	2	5.6
2015	20	831	92.8	2.3	4.9
2015	21	633	93.8	3.2	3
2015	22	738	91.2	3.8	5
2015	23	785	88	4.7	7.3
2015	24	673	92.6	1.2	6.2
2015	25	697	91.8	1.4	6.7
2015	26	939	90.3	2.7	7
2015	27	897	95.4	1.4	3.1
2015	28	1011	95.5	1.7	2.8
2015	29	502	97.4	1	1.6
2015	30	697	94	4.4	1.6

2.6. Practical Considerations

2.6.1. Numerical Computation Considerations

The binary snow cover algorithm is simple from the mathematical standpoint. The algorithm is not computationally intensive as it does not involve iterations complex physical models or inversion of large matrices.

2.6.2. Programming and Procedural Considerations

None.

2.6.3. Quality Assessment and Diagnostics

The procedure has been developed to acquire IMS data and in situ observations data in an automated fashion and match the two datasets with the derived gridded snow cover data on a daily basis. This procedure is applied routinely for the VIIRS snow retrievals. A similar approach will be implemented to monitor the quality of Binary Snow products from MetImage and ABI.

2.6.4. Exception Handling

The developed software is designed to handle a variety of processing problems, including bad and missing data and fatal errors. In the event that processing problems prevent the production of useful binary snow retrievals, error flag will be written to the output product file as metadata.

2.7. Validation

As stated in section 2.5.3., validation of the Binary Snow algorithm and of the corresponding snow product is performed using various approaches and techniques. Qualitative assessment of the product accuracy and consistency is performed through visual comparison of the snow maps with matching true color imagery and with automated snow cover products derived from similar satellite sensors (e.g., MODIS, AVHRR). Quantitatively the product accuracy is evaluated through its comparison with snow maps generated within NESDIS Interactive Multisensor Snow and Ice Mapping System (IMS) and with in situ snow depth reports from ground-based stations.

The results of quantitative validation of the VIIRS-based binary snow product demonstrated its high accuracy. It agrees on the presence/absence of the snow cover to within 92.5% with the station data and matches IMS data in over 95% of retrievals. This implies that the algorithm fully satisfies the accuracy requirement of 90% correct snow/no snow typing. We expect a similar performance of the Binary Snow cover algorithm with MetImage and ABI data.

3. ASSUMPTIONS AND LIMITATIONS

3.1. Performance Assumptions

The principal assumption in the snow fraction retrievals is that the cloud mask used in the retrievals as an external product is accurate. Missed clouds are most likely to be labeled as snow-covered by the binary snow cover algorithm and thus may cause false snow identifications.

Forest cover, cloud and topographical shadows complicate accurate snow identification and mapping. Therefore, in the forested regions as well as in the mountains the accuracy of snow maps may degrade.

3.2. Potential Improvements

The current snow identification algorithms can be generally improved by tuning the algorithm including both the spectral test and consistency test parameters. Accurate characterization of the background visible reflectance of the snow-free land surface, if available, can substantially facilitate discrimination of snow free and snow covered scenes and thus improve the snow cover mapping.

4. REFERENCES

GSegDPS (2019) Joint Polar Satellite System (JPSS) Ground Segment Data Product Specification, https://www.jpss.noaa.gov/assets/pdfs/technical_documents/474-01543_JPSS-GSegDPS_A.pdf

Hall D.K., G.A.Riggs and V.V. Salomonson (2001), Algorithm Theoretical Basis Document (ATBD) for the MODIS Snow and Sea Ice-Mapping Algorithms. <http://modis-snow-ice.gsfc.nasa.gov/atbd.html>.

JPSS (2015) Joint Polar Satellite System (JPSS) Calibration/Validation Plan for Binary Snow Cover Product , Version 1.2 DRAFT, 29 p.

Key, J. R., R. Mahoney, Y. Liu, P. Romanov, M. Tschudi, I. Appel, J. Maslanik, D. Baldwin, X. Wang, and P. Meade, 2013, Snow and ice products from Suomi NPP VIIRS, J. Geophys. Res. Atmos., 118, doi:10.1002/2013JD020459.

Romanov P., G. Gutman and I. Csiszar (2000) Automated monitoring of snow cover over North America with multispectral satellite data, Journal of applied Meteorology, 39, 1866-1880.

Romanov P., D. Tarpley, G. Gutman and T.Carroll (2003) Mapping and monitoring of the snow cover fraction over North America. Journal of Geophysical Research, D108, 8619, doi:10.1029/2002JD003142, 2003

Romanov P. (2014) Global 4km Multisensor Automated Snow/Ice Map (GMAI): Algorithm Theoretical Basis Document. NOAA NESDIS, September 2014, 60 p, online at http://www.star.nesdis.noaa.gov/smcd/emb/snow/documents/Global_Auto_Snow-Ice_4km_ATBD.pdf

VIIRS (2012) Visible Infrared Imaging Radiometer Suite (VIIRS) Sensor Data Record (SDR) User's Guide, NOAA Technical Report NESDIS 142, Washington D.C., 10 September, 2013, online at http://www.star.nesdis.noaa.gov/smcd/spb/nsun/snpp/VIIRS/VIIRS_SDR_Users_guide.pdf
